

Sonogenetics is a novel antiarrhythmic treatment

Yang Li^{a,b}, Xingang Wang^b, Jianzhong Guo^b, Yong Wang^{c,d}, Vladimir Zykov^c, Eberhard Bodenschatz^{c,d,e,f}, and Xiang Gao^{b,c,1}

^aSchool of Science, Beijing University of Posts and Telecommunications, Beijing, China; ^bSchool of Physics and Information Technology, Shaanxi Normal University, Xi'an, China; ^cLaboratory for Fluid Physics, Pattern Formation and Biocomplexity, Max Planck Institute for Dynamics and Self-Organization, Göttingen, Germany; ^dDZHK (German Center for Cardiovascular Research), Partner Site Göttingen, Göttingen, Germany; ^eInstitute for Dynamics of Complex Systems, University of Göttingen, Göttingen, Germany; ^fLaboratory of Atomic and Solid-State Physics and Sibley School of Mechanical and Aerospace Engineering, Cornell University, Ithaca, New York, United States of America

An implantable cardioverter defibrillator (ICD), a widely used treatment for patients at risk of sudden cardiac death due to cardiac arrhythmias, is invasive and compromises patients' quality of life. To eliminate cardiac arrhythmias, the sonogenetic treatment technique proposed here focuses transthoracic ultrasound at the heart, stretches the tissue in the focal area, and thereby controls stretch-activated ion channels genetically expressed on the cell membrane of cardiac myocytes. In contrast to anchoring the implanted ICD electrode at a fixed position in the myocardium, the position of the ultrasound focal area, and thus the area of manipulation of the myocardium can be dynamically selected in size and position to eliminate arrhythmias. Our simulations predict optimal control of malignant electrical excitations of the heart. The intensity and frequency of ultrasound are harmless to humans and well below the limits established by the U.S. Food and Drug Administration. The sonogenetic treatment is painless in all cases. The proposed sonogenetic arrhythmia control is ideally suited for the treatment of cardiac arrhythmia.

Sonogenetics | Defibrillation | Arrhythmia control | Ultrasound

Cardiac arrhythmias can lead to stroke, heart failure, or sudden death (1–3). The established medical treatment for cardiac arrhythmias is the implantable cardioverter defibrillator (ICD) (4). The wires of the ICD are passed through a vein and terminate in electrodes that are anchored in the heart muscle. The ICD device itself is installed under the skin and measures the electrical activity of the heart. If cardiac arrhythmias are detected, the ICD delivers high-voltage electrical shocks to the heart muscle, resetting the electrophysiological system and restoring a normal heartbeat. This invasive and potentially very painful treatment carries significant risks, such as infection at the implant site and damage to blood vessels from the ICD wires. It adversely affects the patient's quality of life (5–7). Therefore, cardiologists wish for less invasive antiarrhythmic treatments (8).

Sonogenetics finds its first use in the non-invasive regulation of excitable cells, such as neurons (9–11) since the seminal work by Ibsen et al. in 2015 (12). Neurons are excited or inhibited by the ionic current from stretch-activated ion channels (SACs). SACs' opening probability changes with the membrane tension (13–15), which can be non-invasively controlled by harmless transthoracic ultrasound (16, 17).

Here we propose sonogenetics to treat malignant electrical excitations of the heart, i.e. arrhythmia, without invasive electrical connections. We establish with in-silico experiments procedures that can be accomplished with wearable medical devices. We model the relationship between ultrasonic radiation pressure and SACs' current and study the effect of SACs' current in two ventricular models. Our results show that sonogenetics can effectively eliminate tachycardia and fibrillation, corresponding to the electrophysiological patterns of rotors

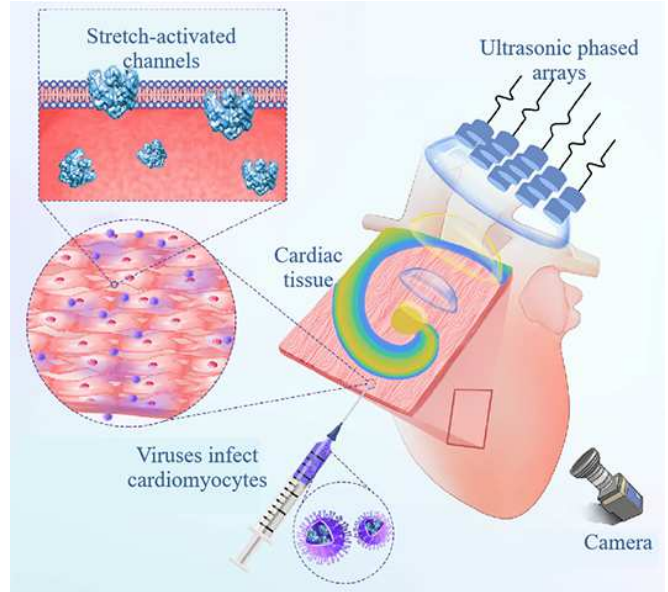


Fig. 1. Proposed experiment to demonstrate sonogenetics for treatment of cardiac arrhythmia. Middle: a piece of genetically altered cardiac tissue is explanted from a sacrificed animal to be studied ex vivo. Bottom and Left: virions transfect the cardiac tissue in vivo, and stretch-activated ion channels are expressed on the cardiomyocyte membranes. Top right: ultrasonic phased arrays focus sound waves with spatial and temporal control. Blue and yellow indicate the pressure of the ultrasound. The ultrasonic radiation pressure controls the stretch-activated ion channels. Within the ultrasonic focus, cardiomyocytes are excited or inhibited, and arrhythmia is eliminated (illustrated by a spiral wave). Bottom right: A fluorescence imaging from voltage-sensitive dyes can be used to verify sonogenetic antiarrhythmic control.

and electric turbulence, respectively (18, 19). The ultrasound we use in the simulations is within the U.S. Food and Drug Administration (FDA) safety standard. We use two common

Significance Statement

Sonogenetics is an excellent candidate for the safe treatment of cardiac arrhythmia. Ultrasound focused spatially and temporally on an area of the myocardium slightly stretches the tissue, thereby activating ion channels that have been genetically incorporated into cardiomyocytes. We predict that spatiotemporal control of these ion channels by ultrasound will interrupt the erratic electric excitations of the heart and noninvasively eliminate or prevent cardiac arrhythmias.

Author contributions: X.G. designed the research. Y.L. and X.G. performed the research and wrote the manuscript. X.W., J.G., Y.W., V.Z. and E.B. contributed to the data analysis. Y.W., V.Z., and E.B. edited the manuscript.

The authors declare no conflict of interest.

¹To whom correspondence should be addressed. E-mail: gaoliang.gnaixog@gmail.com

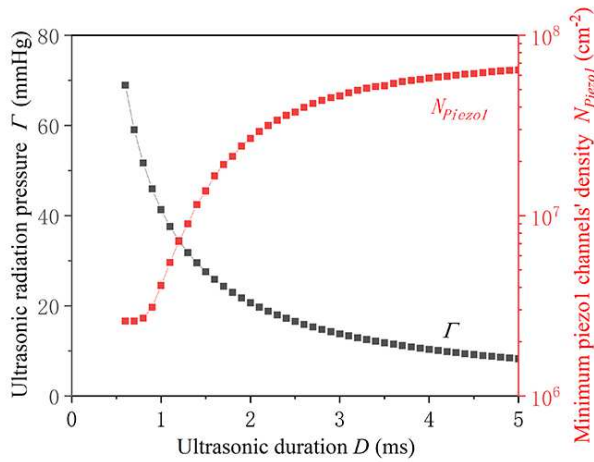


Fig. 2. Relationship between ultrasonic duration D and radiation pressure Γ according to the FDA standard (33) (solid black line). The minimum Piezo1 channels density N_{Piezo1} above which the action potential can be excited (red dashed line) when the values of Γ and N_{Piezo1} are on the solid black line.

SACs (the Piezo1 channel (20) and the MscL channel (21)) in two representative cardiac models (Fenton-Karma three-variable model (22) and Luo-Rudy I model (23)), respectively and find the same results. The independence of the particular ion channel or model used points to the robustness of sonogenetic arrhythmia control. Sonogenetics is a prime candidate for the non-invasive and harmless treatment of malignant electrical excitations of a person's heart.

Results

In-silico experiment. Our research is based on in-silico experiments. They capture all parts of an envisioned ex-vivo experiment, see Fig.1. Each part has been implemented respectively: genetically modified cardiac tissue of a guinea pig or rabbit (24), expression of stretch-activated ion channels (25), ultrasonic phased arrays focusing (26), and fluorescence image recording (27).

We focus our investigation mostly on Piezo1 channels as SACs because they have three advantages: (i) Piezo1 channels are abundant in the human body in general and are up-regulated in failure heart as an adaptive response to meet the mechanical load of the heart under pathological or aging conditions (28, 29); (ii) Piezo1 channels are genetically homologous with humans, and severe immune rejection during transfection can be avoided (30); (iii) they are the most mechanosensitive SAC channel known (31) which can be activated by low-intensity ultrasound (32) (see SI, Fig. S1 c).

Proof of concept. To explore which radiation pressure and pulse duration of the ultrasound is needed to trigger waves of electrical excitation in genetically modified tissue we first studied a ring (circular cable) of cardiac tissue. We simulate the membrane potential changes on every node along the ring. The spatial-peak temporal-average intensity (ISPTA) of medical pulsed ultrasound applied to the heart should not exceed 430 mW/cm² according to a FDA standard (33). The ISPTA is the product of ultrasonic intensity I_0 with the duration D of application ($ISPTA = I_0 D$). The magnitude of the ultrasonic

radiation pressure Γ is controlled by the ultrasonic intensity I_0 : $\Gamma = 2I_0/c$ (see SI, Supplement), where $c = 1561.3m/s$ is the speed of ultrasound in cardiac tissue. The black line and symbols in Fig. 2 represent the ultrasonic radiation pressure Γ as a function of D for $ISPTA = 430$ mW/cm². The red line and symbols in Fig. 2 represent the minimum Piezo1 channels density N_{Piezo1} required to excite the action potential at a node of the ring. When the Piezo1 channels' density exceeds this value, Piezo1 channels' current generated by ultrasonic radiation pressure excites the node to generate a propagating action potential (see SI, Fig. S2). Please note, that during and immediately after a node fires the cardiomyocytes cannot be excited by any external stimulus. This property is called refractoriness, and the period where the cardiomyocyte is unresponsive to stimulation is called the refractory period. In the following, we use exactly this property to locally create refractory tissue which as we will show below allows us to stop arrhythmia and fibrillation.

Fibrillation termination by global ultrasound. We first demonstrate that global ultrasound stimulation can reset cardiac electrical signals to eliminate fibrillation. A global defibrillation is also what an ICD performs. Figure 3 (and also in Movie S1) shows a snapshot of self-sustained electric turbulence of the cardiac tissue, i.e. fibrillation. At $t = 0$ ms a global ultrasound stimulation of $D = 1ms$ is applied. At $t = 20ms$, the whole tissue is excited – refractoriness blocks propagation of electrical excitation. At $t = 50ms$, with the change of action potential, the membrane potentials of the simulation nodes return to the resting potential. At $t = 145ms$, the cardiac tissue is reset to the normal excitable state, and turbulence is eliminated. Under the FDA requirement for the ISPTA, we use $D = 1ms$ and $\Gamma = 41.35mmHg$.

Except for complying with the ISPTA, FDA also uses the mechanical index (MI) and the thermal index (TI) to require the safety of ultrasonic regarding cavitation and thermal effects, respectively (34). The mechanical index MI is the ratio of the peak negative pressure p in MPa and the square root of the ultrasonic frequency f in MHz . The FDA-approved maximum value of the mechanical index $MI_{max} = 1.9$. The thermal index TI for soft tissues is defined as the product of $ISPTA$ in $[mW/cm^2]$ and the ultrasound focus area A in cm^2 and the ultrasonic frequency in MHz , divided by 210. The FDA-approved maximum value of the thermal index $TI_{max} = 6$. Thus, the ultrasonic frequency f is an important parameter for both MI and TI . Considering $p = \sqrt{2\rho c I_0}$ (the cardiac tissue density $\rho = 1081kg/m^3$) and $\Gamma = 2I_0/c$, to satisfy $MI(f) < MI_{max}$, the minimum ultrasonic frequency $f_{min}^{MI} [MHz] = 0.35\Gamma [mmHg]/1.9^2$. To satisfy $TI(f) < TI_{max}$, the maximum ultrasonic frequency $f_{max}^{TI} [MHz] = 2.93/A [cm^2]$. Therefore, we need a suitable ultrasonic frequency range $[f_{min}^{MI}, f_{max}^{TI}]$ to simultaneously meet the FDA requirement for MI and TI .

In our simulations for global termination of fibrillation, we find that $f_{min}^{MI} = 4.01MHz$ and $f_{max}^{TI} = 0.03MHz$. $f_{min}^{MI} > f_{max}^{TI}$, which means that there is no ultrasonic frequency range for the global ultrasound stimulation that can meet both the FDA requirements for MI and TI . The reason is that the ultrasonic focus area A is too large. Therefore we need different approaches that reduce A and thus increase f_{max}^{TI} so that we can have a suitable ultrasonic frequency range under all FDA requirements.

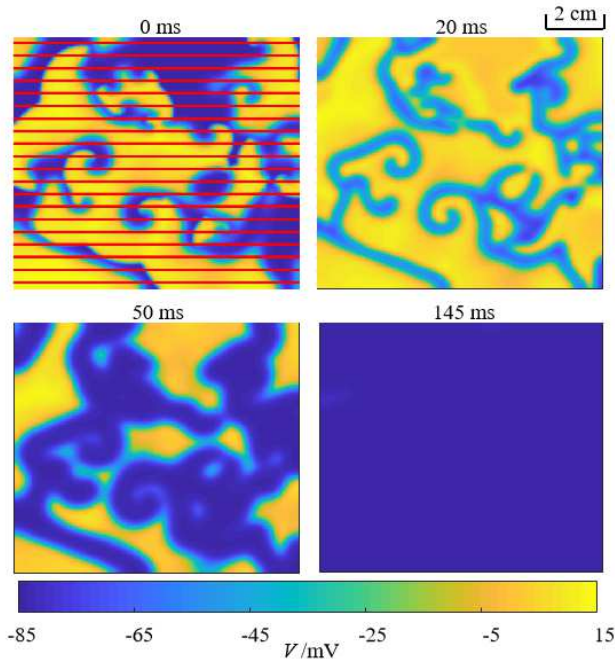


Fig. 3. Membrane potential V snapshots in a $10\text{cm} \times 10\text{cm}$ homogeneous cardiac tissue showing the process of global defibrillation. Ultrasound is applied to the whole tissue (indicated by the red shadow), i.e. globally for one millisecond. The ultrasonic radiation pressure $\Gamma = 41.35\text{mmHg}$, and Piezo1 channels density $N_{\text{Piezo1}} = 1 \times 10^7 \text{cm}^{-2}$. After 145ms the electric turbulence subsides and normal rhythm can resume. An example is shown in Movie S1.

Control by ultrasonic stripe sweeping. To reduce the ultrasonic focus area A and thus comply with all FDA requirements, we propose the local ultrasonic stimulation. Using an ultrasonic phased array, a locally focused stripe can be swept across the tissue. As we show exemplary below this efficiently stops electric turbulence in the cardiac muscle. As shown in Fig. 4 (and also in Movie S2), the ultrasound is focused as a stripe (red shadow) of width 0.05cm and ultrasonic radiation pressure $\Gamma = 41.35\text{mmHg}$ sweeping at 0.05cm/ms across the patch. As shown with the snapshots in Fig. 4, at $t = 0\text{ms}$, the ultrasonic stripe is located on the left edge of the tissue. Then, it is swept with uniform and constant amplitude and velocity from the left side of the patch to the right. The nodes in the area swept by the ultrasonic stripe are excited and become refractory, so turbulence is blocked and gradually disappears (see Fig. 4 at 50ms and 150ms). At $t = 355\text{ms}$, electric turbulence has completely been eliminated and the cardiac tissue returns to the excitable state. In addition, local ultrasonic stimulation can disperse the ultrasound energy spatially to avoid excessive thermal effects. We calculate that $f_{\text{min}}^{\text{MI}} = 4.01\text{MHz}$ and $f_{\text{max}}^{\text{TI}} = 5.86\text{MHz}$, i.e., MI and TI both meet the requirements of the FDA when the ultrasonic frequency is between 4.01MHz and 5.86MHz . Finally, we test the range of parameter selection that can successfully eliminate turbulence under the same initial condition as in Fig. 4 (see SI, Fig. S3).

Unlike the hard contact of traditional ICD electrodes, spatiotemporal selective stimulation of ultrasonic phased arrays is a novel and practical excitation method. This method can change the focus position in real-time and dynamically sweep

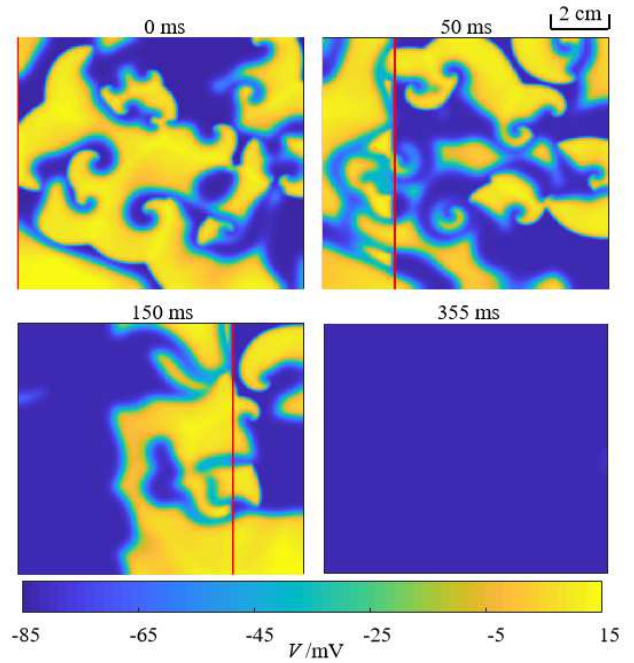


Fig. 4. Membrane potential V snapshots of defibrillation by a moving stripe-shaped ultrasound. Ultrasound is continuously focused on a 0.05cm wide stripe (indicated by the red line), which moves from the left of the tissue to the right at a speed of 0.05cm/ms . The ultrasonic radiation pressure $\Gamma = 41.35\text{mmHg}$, and Piezo1 channels density $N_{\text{Piezo1}} = 1 \times 10^7 \text{cm}^{-2}$. A video of turbulence being swept is shown in Movie S2.

turbulence away, which ICD electrodes cannot do.

Overriding the spiral wave by ultrasonic series. The occurrence of spiral waves in the heart is clinically corresponding to tachycardia and may turn into lethal fibrillation. In excitable media such as the heart, high-frequency serial waves drive slow-frequency waves out of the medium boundary (35). According to this principle, ICD electrodes are used clinically to generate high-frequency serial waves that override spiral waves, referred to as anti-tachycardia pacing (36). We propose to use ultrasound instead of ICD electrodes to generate high-frequency target waves non-invasively. Fig. 5 (and Movie S3) show ultrasound generates high-frequency target waves (8Hz) to displace the slow-frequency spiral wave (6.3Hz) out of the tissue boundary. We use the Jacobian-determinant method (37) to mark the position of the tip of the spiral wave (white dot in Fig. 5). If the tip leaves the tissue, it can be determined that the spiral wave will disappear. At $t = 0\text{ms}$, the ultrasound is pulsed on a circular area (red shadow) to generate target waves. Then, the spiral wave is gradually pushed to the boundary by the ultrasonic target wave, and the tip also moves to the boundary (as shown in the 300ms and 600ms snapshots in Fig. 5). At $t = 730\text{ms}$, the tip of the spiral wave leaves the tissue, and then the spiral wave gradually disappears. After the spiral wave is eliminated, we stop the ultrasonic target wave stimulation, and the cardiac tissue returns to the excitable state. In this case, according to the requirement for the ISPTA, we use $D = 0.1 \times 8 = 0.8\text{ms}$ and $\Gamma = 51.68\text{mmHg}$. Then, we calculate that $f_{\text{min}}^{\text{MI}} = 5.01\text{MHz}$ and $f_{\text{max}}^{\text{TI}} = 5.83\text{MHz}$.

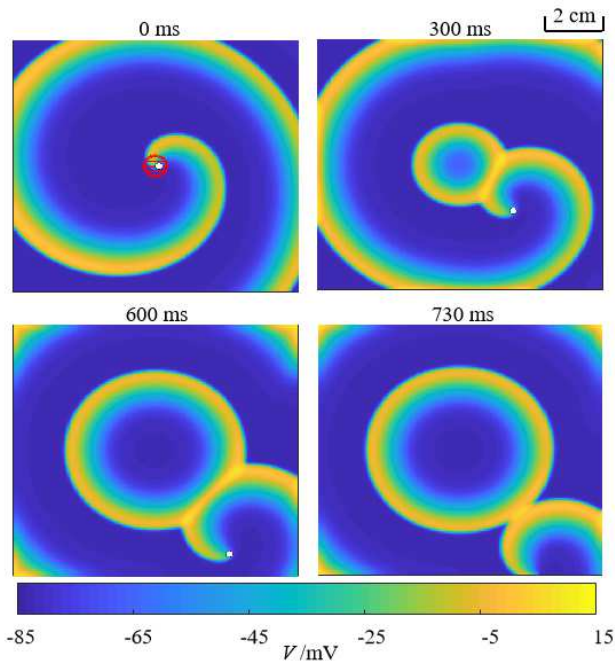


Fig. 5. Membrane potential V snapshots of high-frequency target wave series generated by ultrasound driving the spiral wave away. The spiral wave rotates at a frequency of 6.3Hz . The white dot indicates its tip. The ultrasound is pulsed on a circular area (indicated by a red shadow) with a radius of 0.4cm in the center of the tissue. The pulse frequency is 8Hz , and each pulse lasts 0.1ms . The ultrasonic radiation pressure $\Gamma = 51.68\text{mmHg}$. The Piezo1 channels density $N_{\text{Piezo1}} = 1 \times 10^7 \text{cm}^{-2}$. A video of the spiral wave being overridden is shown in Movie S3.

The generation of target waves by ultrasound can circumvent some disadvantages of ICD electrodes. According to the eikonal relation of the excitable medium (38), the target wave must have a large enough excitable radius to propagate. Therefore, the electrodes of the ICD must be large enough to propagate the target wave, which may cause vascular damage when implanted. In addition, these electrodes are hard contacted onto the surface of the heart and may fall off when the heart beats, leading to treatment failure. Ultrasonic phased arrays can change the size and position of the focal area in real-time from afar and can effectively prevent these shortcomings of ICD electrodes.

Ultrasonic target waves can effectively eliminate spiral waves. However, the frequency of target waves will not continuously respond to the increasing frequency of the ultrasonic pulses. The frequency of ultrasonic target waves has an upper limit, at which phase-locking phenomena change (see SI, Fig. S4). Therefore, the approach of overriding by ultrasonic series is only applicable for slow spiral waves.

Pulling the spiral wave away by ultrasonic ring. To eliminate spiral waves at any frequency, we use a new approach. We use a ring-shaped ultrasonic focal area to create a ring-shaped refractory area in the cardiac tissue. As shown in Fig. 6 (and also in Movie S4), at $t = 0\text{ms}$, the ultrasonic ring (red ring) is focused to the right of the spiral tip to generate a ring-shaped refractory area. The spiral wave cannot pass through this refractory area and will revolve around it, which we call pinning. Then, we slowly move the ultrasonic ring outside

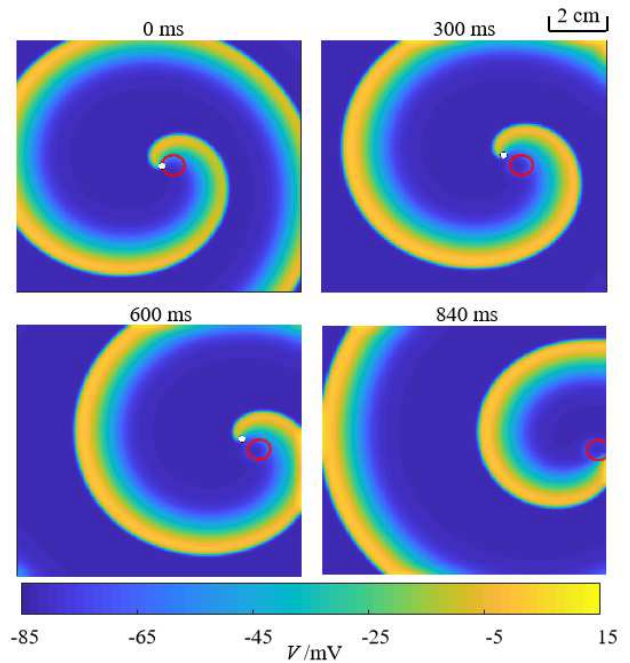


Fig. 6. Membrane potential V snapshots of an ultrasonic ring pinning and pulling the spiral wave away. The white dot indicates the tip of the spiral wave. The ultrasound is pulsed on a ring (indicated by the red ring). The width of the ring is 0.025cm , the radius of the inner circle is 0.4cm , and the moving speed is 0.005cm/ms . The pulse frequency is 200Hz , and each pulse lasts 0.5ms . The ultrasonic radiation pressure $\Gamma = 41.35\text{mmHg}$, and Piezo1 channels density $N_{\text{Piezo1}} = 1 \times 10^7 \text{cm}^{-2}$. A video of the spiral wave being pulled away is shown in Movie S4.

the tissue boundary, and the pinned spiral wave is pulled out (as shown in the 300ms , 600ms , and 840ms snapshots in Fig. 6). In this case, the ultrasonic ring moves 0.025cm to the right every 5ms . In the process of the ultrasonic ring movement, some areas will be stimulated twice by ultrasound. To meet the FDA's requirement for the ISPTA, we set the ultrasonic pulses to stimulate once every 5ms , each lasting 0.5ms . So, nodes in the tissue are stimulated by ultrasound for a maximum of 1ms . Therefore the ISPTA is within the FDA's requirement. In addition, due to the small area of the ultrasonic ring, there is a wide ultrasonic frequency range ($f_{\text{min}}^{\text{MI}} = 4.01\text{MHz}$, $f_{\text{max}}^{\text{TI}} = 45.22\text{MHz}$). The phase diagram of the ultrasonic ring's moving velocity and direction that can successfully eliminate this spiral wave is shown in SI, Fig. S5.

Leading the spiral wave out by ultrasonic fast channel staircase.

To eliminate the spiral wave faster, we propose to use spatiotemporally selective ultrasound to create a "fast" channel that leads the spiral wave out. Here, we use a staircase-shaped fast channel to shorten the focusing duration of the ultrasound at the same position. At $t = 0\text{ms}$, we add the first stair around the tip of the spiral wave. Then, the ultrasonic area moves 0.05cm to the right every 13ms . After each position update, the ultrasound stimulates for 1ms , and the upper boundary of the ultrasonic stair is on the same ordinate as the tip of the spiral wave. As shown in the 52ms , 104ms , and 175ms snapshots in Fig. 7 (and also in Movie S5), the tip gradually moves out of the tissue boundary along ultrasonic stairs. In this case, the ultrasound stimulation is mobile, and each node is stimulated within 1ms . The ISPTA

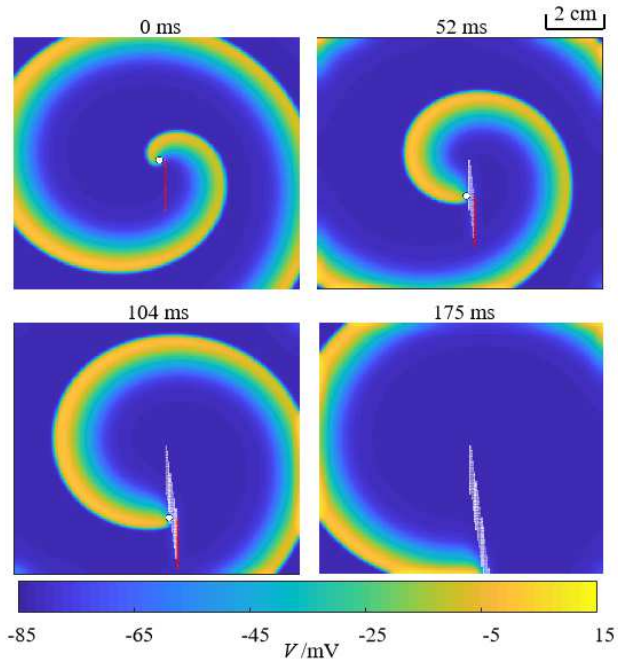


Fig. 7. Membrane potential V snapshots of ultrasonic stairs leading the spiral wave out of the tissue. The white dot indicates the tip of the spiral wave. The ultrasound is pulsed on an area 2cm long and 0.05cm wide (indicated by the red line). The white shadow indicates the areas focused by ultrasound at the previous moments. Every 13ms , the ultrasonic area moves to the lower right to form stairs, and ultrasonic stimulation is performed for 1ms . The tip of the spiral wave moves downward along ultrasonic stairs. The ultrasonic radiation pressure $\Gamma = 41.35\text{mmHg}$, and Piezo1 channels density $N_{\text{Piezo1}} = 1 \times 10^7\text{cm}^{-2}$. A video of the spiral wave being led out is shown in Movie S5.

meets the requirement of the FDA, and we calculate that $f_{\min}^{MI} = 4.01\text{MHz}$ and $f_{\max}^{TI} = 29.30\text{MHz}$.

The above two mechanisms eliminate the spiral wave by directing the tip outward. The success of these two approach is due to the spatiotemporally selective stimulation by ultrasound, which cannot be achieved with ICD electrodes.

Discussion

Proof of model independence. To demonstrate that our results are model-independent, we reproduce the main results using the guinea pig Luo-Rudy I model (see SI, Supplementary text) (39) with MscL channels' current equation (see SI, Supplementary text, Fig S1 *b* and *d*). These prove that the mechanisms of eliminating turbulence and spiral waves by sonogenetics apply to different SACs and cardiac models (see SI, Fig. S6). Note that these works are used to verify model independence and do not take into account FDA requirements for ultrasound safety.

Side effects of overexpressing Piezo1. Our numerical results in Fig. S7 show that there is no malignant electrical excitation from heartbeats and mechanical trauma when Piezo1 is overexpressed. Based on the experimental data of neonatal rat cardiomyocytes (40), we estimate two limit values of ultrasonic radiation pressures, corresponding to deformations of heart contraction and relaxation, respectively. Assuming the ultrasound radiation pressure changes sinusoidally between

these two limit values during the heartbeats, we demonstrate that no abnormal excitation-contraction coupling occurs. For the same reason, neither can mechanical trauma.

Recently, it was reported in Ref. (41) that Piezo1 is the cardiac mechanosensor that initiates the cardiomyocyte hypertrophic response to pressure overload in adult mice. To prevent the CaMKII-HDAC4-MEF2 hypertrophic signaling pathway, Piezo1 is a potential therapeutic target. Sonogenetics is a useful control because it allows noninvasive and spatiotemporal activation and deactivation of Piezo1.

Advantages over other defibrillation methods . Compared with invasive ICDs, which require wires to be implanted through the vein and fixed electrodes on the endocardium for delivery of electrical shocks, our sonogenetics-based method could place the ultrasonic phased array outside the patient's chest and adjust phases of the array to focus ultrasonic waves on selective areas for effective defibrillation. Compared with optogenetic defibrillation (42–48), which could only illuminate the surface of the heart wall, the ultrasound can penetrate it and control the cardiac excitation transmurally. Compared with previous ultrasonic defibrillation (49–51), our sonogenetics-based method upregulates the density of SACs on the cardiomyocyte membrane, uses the ultrasonic phased array to amplify the ultrasonic intensity only in a small area, and thus terminates arrhythmia harmlessly under FDA safety standards. Recently, a cooling-based method has been proposed (52), but its clinical implementation remains challenging.

Conclusion

We demonstrate competitive advantages and novel mechanisms of sonogenetic arrhythmic control in in-silico experiments. Our numerical results can be accomplished by a combination of existing experimental methods. The potential clinic application can be a wearable device consisting of a Holter monitor and ultrasound transducer phased array for diagnosis and treatment of arrhythmias noninvasively. Our study reveals that sonogenetics is an excellent candidate for harmless antiarrhythmic treatment.

Materials and Methods

According to previous sonogenetics experiments (53), the ultrasonic radiation pressure Γ can be described as (see SI, Supplementary text for the formula derivation):

$$\Gamma = \frac{2I_0}{c}, \quad [1]$$

where I_0 is the ultrasonic intensity; c is the velocity of ultrasound in the medium, which is 1561.3m/s in cardiac tissue. The ultrasonic radiation pressure Γ can be adjusted by changing the ultrasonic intensity I_0 .

To model the transition of Piezo1 channel's states under different pressures, Lewis et al. proposed a four-state model based on experimental data (54). We assume that the ultrasound radiation pressure Γ is the pressure on the Piezo1 channels in the cardiomyocyte membranes. We modify their model to obtain a four-state model for the Piezo1 channel controlled by ultrasonic radiation pressure Γ :

$$\frac{dO_{\text{Piezo1}}}{dt} = a(\Gamma)C + I_1d + hI_2 - (b + c + g)O_{\text{Piezo1}}, \quad [2]$$

where O_{Piezo1} , C , I_1 , and I_2 are the probabilities that the Piezo1 channel is in open, closed and two inactivation states, respectively.

The transition rates between these four states are represented by $a(\Gamma)$, b , c , d , $e(\Gamma)$, f , g , and h , where $a(\Gamma)$ and $e(\Gamma)$ are related to the ultrasonic radiation pressure Γ (see SI, Fig. S1 a). The detailed description and equations of the four-state model for the Piezo1 channel are shown in SI, Supplementary text.

Then, we use the stochastic modeling to describe the current equation of Piezo1 channels:

$$I_{Piezo1} = \bar{g}_{Piezo1} N_{Piezo1} O_{Piezo1}(\Gamma)(V - E_{Piezo1}), \quad [3]$$

where \bar{g}_{Piezo1} and E_{Piezo1} are the maximal conductance of a Piezo1 channel and the reversal potential of 27.3pS and 8.8mV measured in the experiment (55); N_{Piezo1} is the Piezo1 channel's density, which indicates the total number of Piezo1 channels per cm^2 ; O_{Piezo1} is the open probability of Piezo1 channels; V is the membrane potential.

We propose to add Piezo1 channels' current to a normal cardiac model to obtain a cardiac model regulated by sonogenetics. Here we use the Fenton-Karma three-variable model (56) (see SI, Supplementary text) to simulate the electrophysiological activities of human ventricular tissue. This model consists of three variables: the membrane potential V , a fast ionic gate v , and a slow ionic gate w . The three variables are used to produce three independent phenomenological currents: a fast inward inactivation current I_{fi} , a slow time-independent rectifying outward current I_{so} , and a slow inward inactivation current I_{si} . We add Piezo1 channels' current to this model, and the membrane potential equation is as follow:

$$\partial_t V = \nabla(D\nabla V) - \frac{[I_{fi}(V, v) + I_{so}(V) + I_{si}(V, w) + I_{Piezo1}(V, \Gamma)]}{C_m}, \quad [4]$$

where $D = 0.001cm^2/ms$ is the diffusion constant, and $C_m = 1\mu F/cm^2$ is the membrane capacitance. For 2D simulation, no-flux boundary conditions are used. Time evolutions are calculated using an explicit Euler method. The diffusion part in the cardiac model is calculated by the five-point stencil method. The time and space steps are 0.05ms and 0.025cm.

ACKNOWLEDGMENTS. This work is supported by the National Natural Science Foundation of China (Program No. 11727813), Natural Science Basic Research Program of Shaanxi (Program No.2019JQ-163 and NO.2019JQ-810), the Fundamental Research Funds for the Central Universities No. GK202103011, and the Max Planck Society and the German Center for Cardiovascular Research and BMBF through the project IndiHEART. We thank Dr. Amanda H. Lewis from Duke University Medical Center for sharing experimental data about the Piezo1 channel, and Prof. Bingwei Li from Hangzhou Normal University, Prof. Haihong Li, Prof. Junzhong Yang, and Prof. Qionglin Dai from Beijing University of Posts and Telecommunications, Prof. Hong Zhang from Zhejiang University, Prof. Huaguang Gu from Tongji University, Prof. Mengjiao Chen from Leshan Normal University, Prof. Siyuan Zhang from Xi'an Jiaotong University, and Prof. Wei Ren from Shaanxi Normal University for helpful discussions.

- F X Witkowski, L J Leon, P A Penkoske, W R Giles, M L Spano, W L Ditto, and A T Winfree. Spatiotemporal evolution of ventricular fibrillation. *Nature*, 392(6671):78–82, 1998.
- A V Holden. A last wave from the dying heart. *Nature*, 392(6671):20–21, 1998.
- A Garfinkel, Y H Kim, O Voroshilovsky, Z Qu, J R Kil, M H Lee, and P S Chen. Preventing ventricular fibrillation by flattening cardiac restitution. *Proceedings of the National Academy of Sciences*, 97(11):6061–6066, 2000.
- Z Qu, G Hu, A Garfinkel, and J N Weiss. Nonlinear and stochastic dynamics in the heart. *Physics reports*, 543(2):61–162, 2014.
- D Graham-Rowe. Hotwire my heart. *Nature*, 435(7038):14–16, 2005.
- G P Walcott, C R Killingsworth, and R E Ideker. Do clinically relevant transthoracic defibrillation energies cause myocardial damage and dysfunction? *Resuscitation*, 59(1):59–70, 2003.
- A Verma and B L Wilkoff. Intravascular pacemaker and defibrillator lead extraction: a state-of-the-art review. *Heart Rhythm*, 1(6):739–745, 2004.
- R Sankaranarayanan, R Visweswariah, and R J Fox. New developments in cardiac resynchronization therapy. *British Journal of Hospital Medicine*, 74(9):503–509, 2013.
- J Ye and et al. Ultrasonic control of neural activity through activation of the mechanosensitive channel msc1. *Nano letters*, 18(7):4148–4155, 2018.
- C Rabut and et al. Ultrasound technologies for imaging and modulating neural activity. *Neuron*, 108(1):93–110, 2020.
- S Wang and et al. Ultrasonic neuromodulation and sonogenetics: A new era for neural modulation. *Frontiers in Physiology*, 11:787, 2020.

- S Ibsen, A Tong, C Schutt, S Esener, and S H Chalasani. Sonogenetics is a non-invasive approach to activating neurons in *Caenorhabditis elegans*. *Nature communications*, 6(1):1–12, 2015.
- Y C Lin and et al. Force-induced conformational changes in piezo1. *Nature*, 573(7773):230–234, 2019.
- C D Cox and et al. Removal of the mechanoprotective influence of the cytoskeleton reveals piezo1 is gated by bilayer tension. *Nature communications*, 7(1):1–13, 2016.
- A H Lewis and J Grandl. Mechanical sensitivity of piezo1 ion channels can be tuned by cellular membrane tension. *Elife*, 4:e12088, 2015.
- J Wu, A H Lewis, and J Grandl. Touch, tension, and transduction—the function and regulation of piezo ion channels. *Trends in biochemical sciences*, 42(1):57–71, 2017.
- Feasibility and safety of non-invasive ultrasound therapy (niut) on an porcine aortic valve. *Physics in Medicine & Biology*, 65:215004, 10 2020. ISSN 0031-9155. . URL <https://iopscience.iop.org/article/10.1088/1361-6560/aba6d3https://iopscience.iop.org/article/10.1088/1361-6560/aba6d3>
- Q Ouyang, H L Swinney, and G Li. Transition from spirals to defect-mediated turbulence driven by a doppler instability. *Physical Review Letters*, 84(5):1047, 2000.
- J Christoph, M Chebbok, C Richter, J Schröder-Schetelig, P Bittihn, S Stein, I Uzelac, F H Fenton, G Hasenfuß, R F Gilmour, and S Luther. Electromechanical vortex filaments during cardiac fibrillation. *Nature* 2018 555:7698, 555:667–672, 2 2018. ISSN 1476-4687. . URL <https://www.nature.com/articles/nature26001>.
- B Coste and et al. Piezo1 and piezo2 are essential components of distinct mechanically activated cation channels. *Science*, 330(6000):55–60, 2010.
- G Chang, R H Spencer, A T Lee, M T Barclay, and D C Rees. Structure of the mscL homolog from mycobacterium tuberculosis: a gated mechanosensitive ion channel. *Science*, 282(5397):2220–2226, 1998.
- F H Fenton and A Karma. Vortex dynamics in three-dimensional continuous myocardium with fiber rotation: Filament instability and fibrillation. *Chaos: An Interdisciplinary Journal of Nonlinear Science*, 8(1):20–47, 1998.
- C H Luo and Y Rudy. A model of the ventricular cardiac action potential. depolarization, repolarization, and their interaction. *Circulation research*, 68(6):1501–1526, 1991.
- K Wang, P Lee, G R Mirams, P Sarathchandra, T K Borg, D J Gavaghan, and C Bollensdorf. Cardiac tissue slices: preparation, handling, and successful optical mapping. *American Journal of Physiology-Heart and Circulatory Physiology*, 308(9):H1112–H1125, 2015.
- A Reed, P Kohl, and R Peyronnet. Molecular candidates for cardiac stretch-activated ion channels. *Global Cardiology Science and Practice*, 2:19, 2014.
- A Marzo and B W Drinkwater. Holographic acoustic tweezers. *Proceedings of the National Academy of Sciences*, 116(1):84–89, 2019.
- Z Jia and et al. Stimulating cardiac muscle by light: cardiac optogenetics by cell delivery. *Circulation: Arrhythmia and Electrophysiology*, 4(5):753–760, 2011.
- Jianlin Liang, Boshui Huang, Guiyi Yuan, Ying Chen, Fasheng Liang, Huayuan Zeng, Shaolin Zheng, Liang Cao, Deng Feng Geng, and Shu Xian Zhou. Stretch-activated channel piezo1 is up-regulated in failure heart and cardiomyocyte stimulated by angII. *American Journal of Translational Research*, 9:2945, 2017. ISSN 19438141. URL <https://www.ncbi.nlm.nih.gov/pmc/articles/PMC5489894/>.
- F Jiang and et al. The mechanosensitive piezo1 channel mediates heart mechano-chemo transduction. *Nature communications*, 12(1):1–14, 2021.
- Pietro Ridone, Massimo Vassalli, and Boris Martinac. Piezo1 mechanosensitive channels: what are they and why are they important. *Biophysical Reviews*, 11:795–805, 10 2019. ISSN 18672469. . URL <https://link.springer.com/article/10.1007/s12551-019-00584-5>.
- C D Cox, N Bavi, and B Martinac. Origin of the force: the force-from-lipids principle applied to piezo channels. *Current topics in membranes*, 79:59–96, 2017.
- Z Qiu, J Guo, S Kala, J Zhu, Q Xian, W Qiu, and L Sun. The mechanosensitive ion channel piezo1 significantly mediates in vitro ultrasonic stimulation of neurons. *iScience*, 21:448–457, 2019.
- W D O'Brien Jr. Ultrasound–biophysics mechanisms. *Progress in biophysics and molecular biology*, 93(1-3):212–255, 2007.
- C Kollmann and et al. Ultrasound output: thermal (ti) and mechanical (mi) indices. *Ultraschall in der Medizin*, 34(5):422–434, 2013.
- Z Cao, P Li, H Zhang, F Xie, and G Hu. Turbulence control with local pacing and its implication in cardiac defibrillation. *Chaos: An Interdisciplinary Journal of Nonlinear Science*, 17(1):015107, 2007.
- D S Echt and et al. Clinical experience, complications, and survival in 70 patients with the automatic implantable cardioverter/defibrillator. *Circulation*, 71(2):289–296, 1985.
- T C Li and et al. Jacobian-determinant method of identifying phase singularity during reentry. *Physical Review E*, 98(6):062405, 2018.
- F Xie, Z Qu, J N Weiss, and Garfinkel A. Interactions between stable spiral waves with different frequencies in cardiac tissue. *Physical Review E*, 59(2):2203, 1999.
- Z Qu, F Xie, Garfinkel A, and J N Weiss. Origins of spiral wave meander and breakup in a two-dimensional cardiac tissue model. *Annals of biomedical engineering*, 28(7):755–771, 2000.
- B Hissa, P W Oakes, B Pontes, G R Juan, and M L Gardel. Cholesterol depletion impairs contractile machinery in neonatal rat cardiomyocytes. *Scientific reports*, 7(1):1–15, 2017.
- Ze-Yan Yu, Huitao Gong, Scott Kesteven, Yang Guo, Jianxin Wu, Jinyuan Vero Li, Delfine Cheng, Zijiang Zhou, Siiri E. Iismaa, Xenia Kaidonis, Robert M. Graham, Charles D. Cox, Michael P. Feneley, and Boris Martinac. Piezo1 is the cardiac mechanosensor that initiates the cardiomyocyte hypertrophic response to pressure overload in adult mice. *Nature Cardiovascular Research* 2022 1:6, 1:577–591, 6 2022. ISSN 2731-0590. . URL <https://www.nature.com/articles/s44161-022-00082-0>.
- A B Arrenberg, D Y Stainier, H Baier, and J Huiskens. Optogenetic control of cardiac function. *Science*, 330(6006):971–974, 2010.
- T Bruegmann and et al. Optogenetic control of heart muscle in vitro and in vivo. *Nature methods*, 7(11):897–900, 2010.
- B O Bingen and et al. Light-induced termination of spiral wave arrhythmias by optogenetic engineering of atrial cardiomyocytes. *Cardiovascular research*, 104(1):194–205, 2011.

45. R Burton and et al. Optical control of excitation waves in cardiac tissue. *Nature Photonics*, 9 (12):813–816, 2015.
46. E Entcheva and G Bub. All-optical control of cardiac excitation: combined high-resolution optogenetic actuation and optical mapping. *The Journal of physiology*, 594(9):2503–2510, 2016.
47. R Majumder and et al. Optogenetics enables real-time spatiotemporal control over spiral wave dynamics in an excitable cardiac system. *eLife*, 7:e41076, 2018.
48. Rupamanjari Majumder, Vladimir S Zykov, and Eberhard Bodenschatz. From disorder to normal rhythm: Traveling-wave control of cardiac arrhythmias. *Physical Review Applied*, 10: 64033, 2022.
49. A Smalys, Z Dulevičius, K Muckus, and K. Daukša. Investigation of the possibilities of cardiac defibrillation by ultrasound. *Resuscitation*, 9(3):233–242, 1981.
50. D S Echt, A F Brisken, and R E. Riley. Methods and systems for treating arrhythmias using a combination of vibrational and electrical energy: U.s. patent 7,184,830. 2007.
51. R Kohut A and et al. Noninvasive ultrasound cardiac pacemaker and defibrillator: U.s. patent application 12/558,294. 2010.
52. Rupamanjari Majumder, Afnan Nabizath Mohamed Nazer, Alexander V. Panfilov, Eberhard Bodenschatz, and Yong Wang. Electrophysiological characterization of human atria: The understated role of temperature. *Frontiers in Physiology*, 12:639149, 2021. ISSN 1664-042X. . URL <https://www.frontiersin.org/articles/10.3389/fphys.2021.639149>.
53. M D Menz and et al. Radiation force as a physical mechanism for ultrasonic neurostimulation of the ex vivo retina. *Journal of Neuroscience*, 39(32):6251–6264, 2019.
54. A H Lewis, A F Cui, M F Mcdonald, and Grand J. Transduction of repetitive mechanical stimuli by piezo1 and piezo2 ion channels. *Cell reports*, 19(12):2572–2585, 2017.
55. K Saotome and et al. Structure of the mechanically activated ion channel piezo1. *Nature*, 554(7693):481–486, 2018.
56. F H Fenton, E M Cherry, H M Hastings, and S J. Evans. Multiple mechanisms of spiral wave breakup in a model of cardiac electrical activity. *Chaos: An Interdisciplinary Journal of Nonlinear Science*, 12(3):852–892, 2002.